



HAL
open science

Star-poly(lactide)-peptide hybrid networks as bioactive materials

L.V. Arsenie, Coline Pinese, Audrey Bethry, L. Valot, P. Verdie, B. Nottelet, Gilles Subra, V. Darcos, X. Garric

► **To cite this version:**

L.V. Arsenie, Coline Pinese, Audrey Bethry, L. Valot, P. Verdie, et al.. Star-poly(lactide)-peptide hybrid networks as bioactive materials. *European Polymer Journal*, 2020, 139, pp.109990 -. 10.1016/j.eurpolymj.2020.109990 . hal-03491991

HAL Id: hal-03491991

<https://hal.science/hal-03491991v1>

Submitted on 21 Sep 2022

HAL is a multi-disciplinary open access archive for the deposit and dissemination of scientific research documents, whether they are published or not. The documents may come from teaching and research institutions in France or abroad, or from public or private research centers.

L'archive ouverte pluridisciplinaire **HAL**, est destinée au dépôt et à la diffusion de documents scientifiques de niveau recherche, publiés ou non, émanant des établissements d'enseignement et de recherche français ou étrangers, des laboratoires publics ou privés.



Distributed under a Creative Commons Attribution - NonCommercial 4.0 International License

Star-poly(lactide)-peptide hybrid networks as bioactive materials

L. V. Arsenie, C. Pinese, A. Bethry, L. Valot, P. Verdie, B. Nottelet, G. Subra, V. Darcos, X. Garric*

Institut des Biomolécules Max Mousseron (IBMM), Univ Montpellier, CNRS, ENSCM,
Montpellier, France

Keywords: Hybrid polymers, Silylated peptides, Sol-gel crosslinking, Mechanical properties, Biological properties.

ABSTRACT

Poly(lactide) (PLA) is a widely used biomaterial in many biomedical applications. However, it is inert and therefore lacks bioactivity, which is a major drawback in addressing tissue regeneration issues. This work aims to develop new implantable biomaterials composed of PLAs functionalized with bioactive peptides. For that purpose, we set up an original synthesis based on star-PLA bearing triethoxysilyl propyl groups (PLA-PTES) and bifunctional silylated peptides that react together via sol-gel process to create a bioactive network. We demonstrate that the molecular weight of the PLA and the quantity of peptide have a large influence on the crosslinking efficiency, the mechanical properties and the biodegradability of the resulting materials. The presence of peptide increases the crosslinking efficiency of the networks resulting in more rigid networks with stable mechanical properties up to 8 weeks. At last, the potential of

this new type of hybrid biomaterials for soft tissue engineering was demonstrated through cells adhesion assays that showed a significant enhancement of fibroblasts adhesion.

1 Introduction

The recent development in biomedical field has led to the creation of a wide range of biomaterials for regenerative medicine.¹⁻³ In the field of tissue regeneration, new biomaterials tend to promote the interactions with the cellular environment in order to improve either the adhesion of cells and their proliferation or metabolic activity.^{1,4} If well-known biodegradable polymers such as poly(ϵ -caprolactone) (PCL), poly(glycolide) (PGA) and poly(lactide) (PLA), are widely used as material for regenerative medicine due to their biocompatibility and degradability,⁵⁻⁹ the lack of functions on their skeleton limits their interactions with the cellular environment.¹⁰ This is a major disadvantage in tissue engineering applications. The incorporation of bioactive biomolecules such as drugs, proteins or nucleic acids in polymer matrixes by coating or encapsulation could be a solution to this problem.^{11,12} Unfortunately, bioactive molecules are usually rapidly released by desorption and diffusion through the material, which consequently inactivates the polymer matrix. In this context, covalent incorporation of biomolecules into biomaterials is a strategy of choice when sustained bioactivity is required.

Numerous studies focused on the functionalization of degradable polymers with peptides exploring many chemical pathways.^{13,14} As an example, peptides grafting by alkyne azide cycloaddition chemistry has been described on the dibenzocyclooctyne functionalized polymers such as PLA¹⁵ or PEG¹⁶. Alternatively, incorporation of cysteine-containing peptides into the polymer backbone via thiol-ene chemistry is widely described with PCL¹⁷, ethylene glycol dimethylacrylate¹⁸ or four arm-PEG functionalized with norbornene¹⁹. Cysteinyll peptides can also be conjugated to a polymer bearing maleimide^{20,21}, vinyl-sulfone^{22,23}, and acrylate²⁴

functions by Michael addition. Noteworthy, depending on the number of cysteine residues present in the peptides (e.g. one or several), the reaction yields a peptide-polymer conjugate or a three-dimensional network. Whatever the conjugation strategy used, special attention has to be paid on the chemistry of polymerization which should conserve the integrity and the biological properties of the bioactive moiety. Silane chemistry offers the possibility of working in soft conditions to preserve the bioactivity of biomolecules and compatibility with different manufacturing processes. We previously demonstrated that hydrolysis and condensation of alkoxy silane-bearing polymers and peptides could afford, in soft conditions compatible with the side chains of biomolecules, bioactive and modulable hydrogel networks linked through Si-O-Si bonds.^{25,26}

In this study, we extend the scope of this chemoselective crosslinking reaction to biodegradable PLAs functionalized with bioactive peptides, studying different ways to modulate their mechanical properties and their degradability (**Figure 1**). The introduction of a hydroxyl or alkoxy silane group in poly(lactide)s has not been reported so far.²⁷ On the other hand, we have already demonstrated that hybrid bioactive peptides, which bear one²⁸⁻³¹ or several^{32,33} silyl group(s) in controlled position(s) could be synthesized and used as building blocks by sol-gel process, while maintaining their biological properties.

In order to promote the Si-O-Si bonds of the hybrid polymer/peptide network we used a 4-arms star-PLA. We studied the impact of the molecular weight of PLAs and of the concentration of peptides on the crosslinking rate. The mechanical and degradation properties of the different crosslinked hybrid were also evaluated. Finally, we studied the bioactivity of the resulting hybrid networks by quantifying the cellular adhesion on materials containing increasing amounts of peptide.

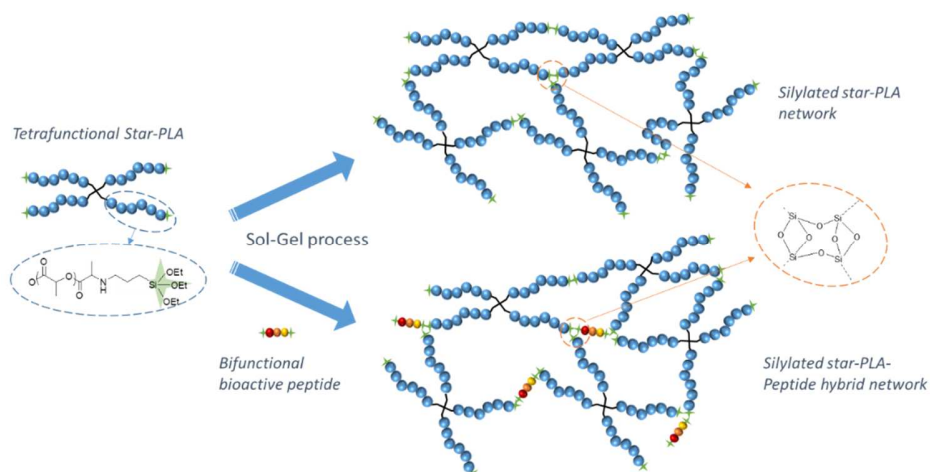


Figure 1. Silylated star-PLA and hybrid silylated star-PLA-peptide networks formation by sol-gel process. (no color needed)

2 Experimental section

2.1 Materials

D,L-lactide was purchased from Purac (Lyon, France). Tin(II) 2-ethylhexanoate ($\text{Sn}(\text{Oct})_2$), pentaerythritol, (3-isocyanatopropyl)triethoxysilane (IPTES), dichloromethane, heptane, toluene, tetrahydrofuran, hydrochloric acid (37%), methanol and phosphate buffer solution (PBS), N,N-diisopropylethylamine (DIEA) and triethylamine were supplied by Sigma Aldrich (St-Quentin Fallavier, France). CellTiter Glo assay was provided by Promega G7571. Fmoc amino acid derivatives, 2-chloro chlorotriyl PS resin, [benzotriazol-1-yloxy(dimethylamino) methylidene]-dimethylazanium hexafluorophosphate (HBTU) and coupling agent were purchased from Iris Biotech GmbH (Marktredwitz, Germany). ClarioStar plate reader was received from BMG Labtek. PrestoBlue® assay was purchased from Invitrogen A13262 (batch 2103456).

2.2 Characterization methods

Size exclusion chromatography (SEC) was conducted on a Shimadzu LC-200AD Prominence system, equipped with a RID-20A refractive index signal detector, a PLgel MIXED-C guard column (Agilent, 5 μ m, 50 \times 7.5 mm), and two PLgel MIXED-C columns (Agilent, 5 μ m, 300 \times 7.5 mm). The polymer was dissolved in THF (5 mg/ml) and the obtained solution was filtered through a Millipore membrane before the injection of 100 μ L into the system. All measurements were performed at 30°C at a flow rate of 1 ml/min. The results were expressed according to a polystyrene calibration. The ¹H-NMR measurements were performed at 300 MHz with an AMX300 Bruker spectrometer using deuterated chloroform as solvent. The chemical signals are expressed in ppm with respect to tetramethylsilane (TMS) signal used as internal reference. The FTIR spectra have been recorded on a Perkin Elmer Spectrum 100 at a scanning rate of 4 cm⁻¹ between 4000 - 550 cm⁻¹.

2.3 Typical procedure for the synthesis of 4-arm star-poly(lactide) of 2 000 g.mol⁻¹ (PLA-2k)

D,L-lactide monomer (15 g, 104 mmol, 14 eq.) and pentaerythritol initiator (1.01 g, 7.4 mmol, 1 eq.) were placed under vacuum 3h before being dissolved in 60 ml of freshly distilled toluene. After complete homogenization, Sn(Oct)₂ catalyst (1.2 g, 2.9 mmol, 0.4 eq.) was added. The ring opening polymerization took place at 110°C for 24h, under inert atmosphere. The product was purified by precipitation with cold heptane and the resulting precipitate was dried under vacuum overnight. The PLA molecular weight was calculated from the atomic ratio between methylene protons of pentaerythritol (δ = 4.13 ppm, s, 2H, C-CH₂-O) and the methyne proton of lactic unit (δ =5.1 ppm, q, 1H, CO-CH(CH₃)-O). Polymers of 10 000 and 12 000 g.mol⁻¹ (PLA-10k and

PLA-12k) have been obtained by varying the amount of initiator as shown in **Supporting Information (Table S1)**. ¹H-NMR (400 MHz, CDCl₃) δ (ppm)= 5.15 (m, CHCH₃); 4.34 (m, CHCH₃-OH); 4.14 (s, C-CH₃-O); 3.5 (s, C-CH₃-OH); 1.54 (m, CHCH₃)

2.4 Synthesis of triethoxysilane-functionalized 4-arm star-poly(lactide)

PLA-2K (10 g, 5 mmol) was placed under vacuum 3h before being solubilized in anhydrous THF under inert atmosphere. IPTES (7.42 g, 30 mmol, 6 eq., i.e. 1.5 eq. per hydroxyl function at the extremity of PLA arm) and Sn(Oct)₂ (1.62 g, 4 mmol, 0.8 eq.) catalyst were then introduced in the solution. The reaction occurred at 85°C for 24h under inert atmosphere. The functionalized polymer (PLA-2k-PTES) was precipitated in cold heptane and kept under vacuum to remove solvent traces. Functionalization yield was determined by the ratio between methyne lactic proton (δ = 5.1 ppm) and the methylene protons linked to triethoxysilane framework (δ = 0.6 ppm). ¹H-NMR (400 MHz, CDCl₃) δ (ppm)= 5.15 (m, CHCH₃); 4.34 (m, CHCH₃-OH); 4.14 (s, C-CH₃-O); 3.83 (m, OCH₂CH₃); 3.5 (s, C-CH₃-OH); 3.17 (m, NH CH₂); 1.54 (m, CHCH₃); 1.2 (m, OCH₂CH₃); 0.64-0.54 (m, CH₂CH₂ Si);

2.5 Peptide synthesis

2.5.1 Common procedures

Fmoc ethylene diamine (EDA) anchoring on 2 chlorotriyl chloride resin

2-Chlorotriyl chloride resin (Loading = 1.6 mmol/g) was placed in a solid-phase peptide synthesis flask fitted with a sintered glass. Fmoc-NH-CH₂-CH₂-NH₂ (2 eq) was anchored to the resin in the presence of DIEA (4 eq) in DMF during 2 hours. After washing steps using the following solvents (2×DMF, 2×DCM/MeOH/DIEA (14/2/1, v/v/v), 3×DCM, 2×DMF, and

2×DCM), Fmoc-NH-CH₂-CH₂-NH-2-Chlorotryl-resin was dried under vacuum for 12 hours. Resin loading was determined by detection of piperidine-dibenzofulvene adduct from pip/DMF deprotection solution at 289 nm. A loading of 0.24 mmol/g was obtained.

Fmoc deprotection

Fmoc-peptidyl-resin was placed in a solid-phase peptide synthesis flask fitted with a glass sintered. Fmoc group was removed by two successive treatments with DMF/piperidine (80/20; v/v) solution of 20 min. Between the two treatments, solution was filtered off and replaced by a new one. Standard washing steps (2×DMF and 2×DCM) were performed at the end of deprotection.

Protected aminoacid coupling step

The appropriate Fmoc-protected amino acid (3eq.) was dissolved in DMF (75% of reactor volume) in presence of HBTU (3eq.) and DIEA (3eq.). This solution was then added to the free N-terminus peptidyl resin and placed under stirring at room temperature for 90 minutes. Standard washing steps were performed afterwards.

2.5.2 Peptide 1 synthesis

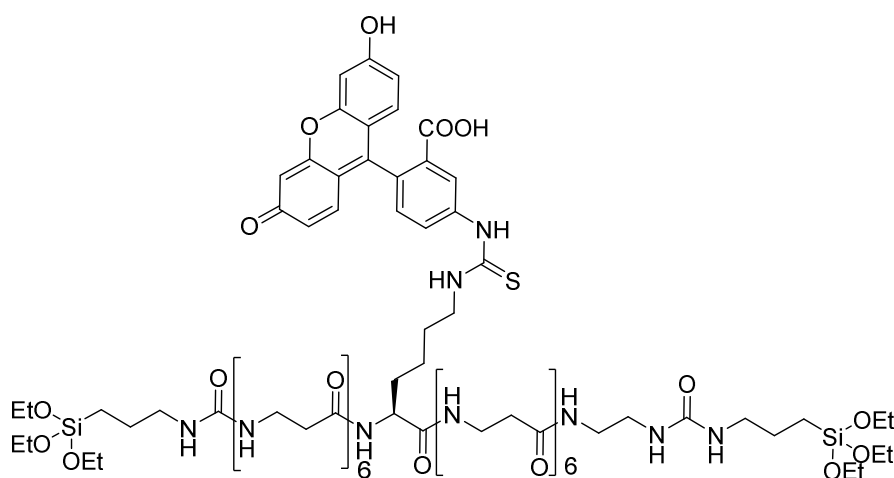


Figure 2. Peptide 1

Peptide **1'** H-(β Ala)₆-Lys(Alloc)-(β Ala)₆-NH-(CH₂)₂-NH₂ was synthesized by standard Fmoc SPPS on Fmoc-NH-CH₂-CH₂-NH-2-Chlorotrityl-resin using successively Fmoc- β Ala-OH and Fmoc-Lysine (Alloc)-OH. At the end of the synthesis, the Alloc protecting group was removed on solid support using a DCM solution containing palladium tetrakis (0.1eq.) and phenylsilane (20eq.) during 30 min under stirring. The deprotection was performed twice in the same conditions. Fluorescein isothiocyanate (2.5eq.) was reacted with lysine side chain using TEA (2.5eq.) at room temperature for 3 hours in DMF. Then the N-Fmoc protecting group was removed as usual, using DMF/pip solution. At last, peptide was cleaved from the resin using a TFA/TIS/H₂O (45/2.5/2.5 v/v/v) solution for 4 hours. TFA was filtered off, concentrated under vacuum. Peptide **1'** was precipitated as TFA salts in diethylether. The crude peptide **1'** was purified by preparative HPLC. Then, it was reacted with 3-isocyanatopropyltriethoxysilane (2.4eq.) in DMF in presence of TEA (4.2eq.). After concentration of the reaction mixture, bis-silylated peptide **1** (**Figure 2**) was obtained by precipitation in diethyl ether recovered peptide **1** with 55 % yield and 90 % purity (**Figure S2**).

2.5.3 Peptide 2 synthesis

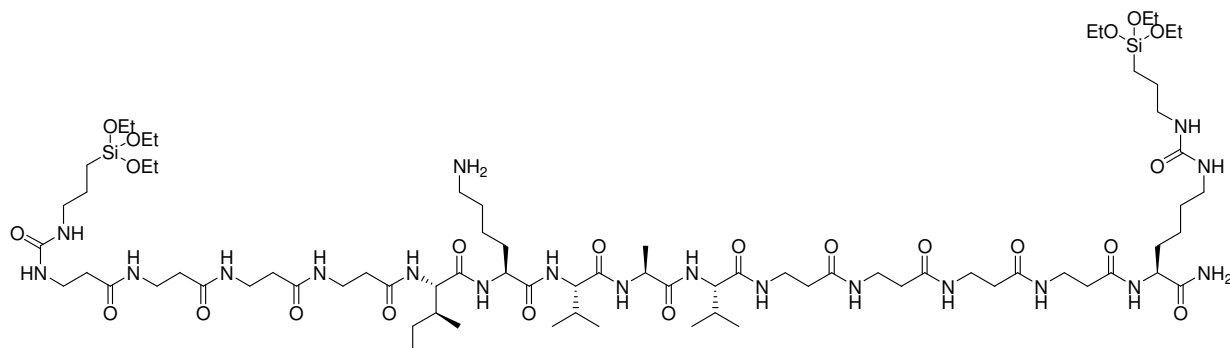


Figure 3. Peptide 2

Peptide **2'** H-(β Ala)₄-IleLys(Nvoc)ValAlaVal-(β Ala)₄-Lys-NH₂ was prepared using the same protocol than peptide **1'** except that Fmoc-Val-OH, Fmoc-Ile-OH, Fmoc-Ala-OH and Fmoc-Lys(Nvoc)OH were used during its synthesis. Peptide **2'** was reacted with 3-isocyanatopropyltriethoxysilane (2.4eq.) in DMF in presence of TEA (4.2 eq.) to yield Nvoc-protect peptide **2''** which was deprotected by UV irradiation at 365 nm during 3 hours. Peptide **2** (**Figure 3**) was obtained by precipitation in diethyl ether recovered with 51 % yield and 99 % purity (**Figure S3**).

2.6 PLA-PTES and hybrid PLA-PTES-Peptide films preparation

1.6 g of PLA-PTES was solubilized in 4 mL of CH₂Cl₂ under magnetic stirring. 50 μ L of HCl/CH₃OH solution (1M) was slowly added in the polymer solution. After 10 minutes of homogenization by stirring, the solutions were placed in silicone molds for solvent evaporation for one week. To assure the complete evaporation of solvent, the molds were placed under vacuum for 48 hours to get PLA films. Hybrid PLA-peptide films were obtained in the same way

except that amounts of bisilylated peptides corresponding to 0.01%, 0.1% and 1% molar ratio, were added in the PLA precursor solution.

2.7 Tensile mechanical assays

Tensile mechanical assays were performed with an Instron 4444 at a crosshead speed rate of 5 mm·min⁻¹. Each sample was analyzed at 37°C in triplicate and Young's modulus (E, MPa), stress at failure (σ_f , MPa), strain at failure (ϵ_f , %) were expressed as the mean value of the three measurements. Young's Modulus was calculated using the initial linear portion of the stress/strain curve.

2.8 Gel fraction evaluation

Gel fractions have been assessed by pouring a film (12.5 mm×5.5 mm×0.5 mm, initial material weight- W_i) in 4 mL of CH₂Cl₂ for 3 hours under slow stirring. The soluble and insoluble fraction were separated by centrifugation (5000 rpm, 7 minutes) and placed in separate tubes. The insoluble and soluble fractions were then dried under vacuum for 24 hours and weighted (weight of insoluble material fraction- $W_{insoluble}$, weight of soluble material fraction- $W_{soluble}$). Each fraction was evaluated from the following equations, after checking that the addition of soluble and insoluble phase was 100% of the initial sample weight:

$$Gel\ fraction\ (\%) = \frac{W_{insoluble}}{W_i} \cdot 100 \quad (1)$$

The results are presented as the mean value of 3 measurements.

2.9 PLA-PTES and hybrid PLA-PTES-peptide films degradation

The films (12.5 mm×5.5 mm×0.5 mm, initial masse- m_i) were immersed in 4 mL of PBS (pH=7.4) at 37°C under continuous stirring. The samples were removed from PBS at different times and samples mass loss, gel fraction and mechanical properties were measured. Samples mass loss was evaluated by weighing samples after drying under vacuum overnight (dry masse- m_d). The masse loss was expressed as the ratio between the mass remained and the total mass:

$$\text{Mass remained/Total mass (\%)} = \frac{m_i - m_d}{m_i} \cdot 100 \quad (2)$$

Samples gel fraction was evaluated by applying the procedure described in 2.7. After removal from PBS and drying under vacuum overnight, the mechanical properties of degraded network films were assessed at 37°C according to the method described in 2.6.

2.10 Cytotoxicity assays

NCTCClone 929 is recommended for the evaluation of *in vitro* cytocompatibility of medical devices according to EN ISO 10993-5. In this study, NCTC-Clone 929 cells (mouse fibroblast cell line (ECACC 85011425)) were cultured in 500 ml of MEM with 5mL of glutamax (1% stabilized glutamine), 50mL of horse serum, and 100U per mL penicillin and streptomycin 100µg per mL. L929 cells (NCTCClone 929) at passage 45 were seeded at 10^4 cells per well (96-well white plate) and allowed to attach for 24 hours. Films were cut into small pieces of 6 cm² (according to ISO 10993-12) and decontaminate under UV (UV-C irradiation at $\lambda = 254$ nm of both film surfaces, followed by 3 washing steps with PBS). Then films and peptide (1mg/ml) were added to L929 cell monolayer and the plates were incubated for 24 hours at 37°C and 5% CO₂. The number of viable cells was obtained by a CellTiter Glo assay (Promega G7571), based

on quantification of the present ATP (which represents metabolically active cells). Phenol was used as positive control and Polyethylene was used as negative control. Results are presented in fluorescent relative unit (FRU) as the mean value of 6 measurements.

2.11 Cell adhesion

Samples (n=3) were exposed to UV-C (Grosseron, Bio-Link 254nm) for 2.5 min per side, placed into 24-well plate and maintained thanks to o-rings. L929 fibroblasts passage 25 were seeded at 6.6×10^4 cells per well. Plates were placed at 37°C and 5% CO₂ for 4 hours. PrestoBlue® assay was used to determine cell viability by using the reducing power of living cells.

3 Results and Discussion

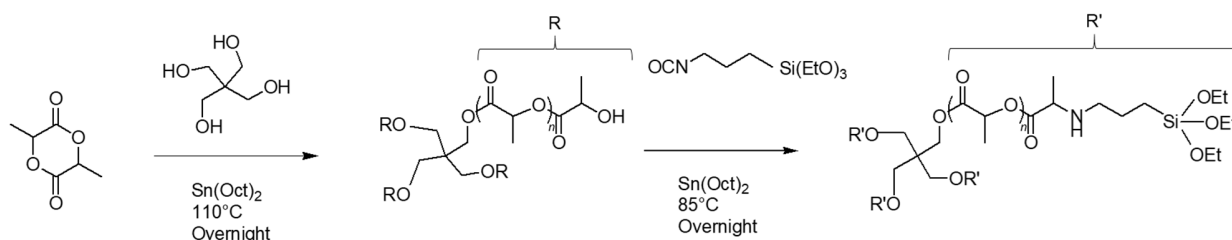


Figure 4. General synthesis of tetra(triethoxysilyl) star-PLA

The synthesis of tetrafunctionalized star-PLA is presented in **Figure 4**. The ring-opening polymerization of D,L-lactide using pentaerythritol as initiator and tin octanoate (Sn(Oct)₂) as catalyst led to star-PLA **3'** with reaction yields up to 80% (**Table 1**). The experimental molecular weights (M_n) of star-PLAs were determined by size exclusion chromatography (SEC) and by ¹H NMR spectroscopy (**Table 1 and Figure S4**) which were closed to the theoretical values. The

functionalization of star-PLA with triethoxysilyl groups was done by reacting isocyanatopropyltriethoxysilane (ICPTES) with hydroxyl end groups of PLA chains, in the presence of Sn(Oct)₂, yielding urethane bonds and silylated star PLA-PTES **3**. The degree of functionalization was calculated by ¹H NMR spectroscopy making the ratio between methyne proton of the lactic units at 5.1 ppm and the methylene protons of triethoxysilane at 0.6 ppm (**Figure S5**). We found that the number of silanes groups per four-arm star-PLA were between 3.45 to 3.99 (**Table 1**) which corresponds to 86 % and 99 % of functionalization. Surprisingly, ¹H NMR analyses showed that the functionalization of star-PLAs **3'** with molecular weights higher than 10 kDa (i.e. **3'b** and **3'c**) resulted in a slight decrease of lactide polymerization degrees of the corresponding silylated star-PLA **3b** and **3c** (**Table 1**). We hypothesized that the Sn(Oct)₂ catalyst used at 0.1 molar eq. per hydroxyl function for the functionalization reaction, generated secondary transesterification reactions leading to a partial depolymerization of star-PLAs.³⁴ This was confirmed by the higher dispersity of the functionalized polymers **3** (**Table 1**). We also tested dibutyltin dilaurate as a catalyst. However, the functionalization rates obtained with this catalyst were lower (~50%) to those obtained with Sn(Oct)₂. In order to reach a better control of the molecular weight of the silylated PLAs, other catalysts or lower Sn(Oct)₂ concentration could be investigated.

Table 1. ¹H-NMR and SEC characterizations of star-PLA and tetrafunctionalized star-PLA

Ref	Polymer	Theoretical molecular weight (g/mol)	Yield %	¹ H-NMR		SEC	
				Molecular weight <i>M_n</i> (g/mol)	Number of PTES groups per PLA chain	Molecular weight <i>M_n</i> (g/mol)	Dispersity (<i>D</i>)
3'a	Star-PLA-2k	2 000	85	2 350	-	2 500	1.36
3a	Star-PLA-2k-PTES	2 900	81	2 850	3.45	3 900	1.92

3'b	Star-PLA-10k	10 000	80	7 600	-	9 900	1.31
3b	Star-PLA-10k-PTES	10 900	84	7 150	3.59	4 700	3.07
3'c	Star-PLA-12k	12 000	87	14 600	-	10 500	1.25
3c	Star-PLA-12k-PTES	12 900	82	10 150	3.99	7 000	2.18
4'	PLA-5k	5 000	89	5 400		7 900	1.75
4	PLA-5k-PTES	5 000	87	4 800	1.43	7 000	1.81

The formation of covalent crosslinked networks from star-PLA-PTES was done using a sol-gel process. First, the hydrolysis of triethoxysilane groups (SiOEt_3) was performed under acidic condition yielding silanol groups (Si-OH), which in a second step condensed into siloxane bonds ($-\text{Si-O-Si}-$) through solvent evaporation, yielding to star-PLA networks. It is worth noting that film formation was not possible with non-modified star PLAs **3'** witnessing that a covalent reticulation of the network can only occurred with star PLA-PTES **3**. Infrared spectroscopy confirmed the appearance of Si-O-Si bonds and the condensation of tetrafunctionalized PLA, showing signal bands at 1635 cm^{-1} and 855 cm^{-1} characteristic to siloxane groups (**Figure S6**).

The impact of the molecular weight (M_n) of the PLA on the network crosslinking efficiency was determined by the estimation of the material gel fraction and by the measurement of the mechanical properties as shown in **Table 2**. Higher M_n star-PLA-PTES **3b** and **3c** formed network with a lower gel fraction, showing the significative influence of M_n on network crosslinking efficiency. Correspondingly, the gel fraction ranged from 99%, 71% and 30% for networks composed of tetrafunctionalized PLA **3a**, **b** and **c** (2k, 10k and 12k), respectively. A high length of the PLA chains seems to hinder the formation of crosslinking bonds and consequently reduces the crosslinking efficiency of the resulting material. The mechanical properties of the biomaterials were then evaluated at 37°C , first comparing films obtained from

star-PLA-PTES **3** and non silylated ones **3'**. However, as already stated, non-functionalized star-PLAs **3'a, b** or **c** were non-filmogenic. Therefore, to get information about the impact of the silane functionalization on the resulting films, we decided to prepare silylated linear PLA **4** with molecular weight $M_n \sim 5000 \text{ g.mol}^{-1}$ and compare it with its non silylated counterparts (**4'**). It is worth noting that each trialkoxysilane moiety may react three times, allowing an efficient crosslinking in the 3 dimensions of space, even if silane groups are only present at both extremities of the polymer. Hydrolysis and condensation of linear silylated PLA **4** enabled the formation of a chemical three-dimensional network more rigid (Young's modulus going from 0.4 to 1.47 MPa), more resistant (stress at failure going from 0.02 to 0.33 MPa) and less deformable (strain at failure going from 653 to 219 %) than the films obtained from unfunctionalized linear PLA **4'** (**Table S7**).

Having demonstrated the interest of siloxane crosslinking for improving the mechanical properties of a PLA network obtained from linear polymers, we then studied the mechanical properties of films obtained from tetrasilylated star-PLA-PTES **3**. The molecular weight of the polymers that formed the three-dimensional chemical network affected its mechanical properties as shown in **Table 2**. As the molecular weight of the polymers increased (2k, 10k, 12k), we observed a decrease of the young modulus (24.3, 3.3 and 1.0 MPa) and of the stress at failure (1010, 380 and 5 MPa) along with an increase of the strain at failure (9.1, 16.4 and 28.7 %). These results highlight the wide range of mechanical properties that can be obtained with these PLA networks by the simple control of the pre-polymer molecular weight. This could be of clear advantage for matching the biomaterials properties with the ones of target tissues to be regenerated.

Table 2 Mechanical properties at 37°C of PLA-PTES films and PLA-PTES-peptide hybrid films: the mean value of Young's Modulus (E, MPa), stress at failure (σ_f , kPa) and strain at failure (ϵ_f , %)

Films composition	Gel fraction (%)	E (MPa)	σ_f (kPa)	ϵ_f (%)
PLA-2k-PTES 3a	99	24.3 ± 3.4	1010 ± 409	9.1 ± 2.2
PLA-10k-PTES 3b	71	3.3 ± 0.1	380 ± 9.7	16.4 ± 0.5
PLA-12k-PTES 3c	30	1.0 ± 0.5	5 ± 1	28.7 ± 4.7
PLA-12k-PTES 3c -0.1% peptide 1	82	3.8 ± 0.7	178 ± 25	9.9 ± 3.1

Thanks to silane chemistry, the introduction of additional biological properties of the network proved to be straightforward.^{25,33} Indeed, silylated peptides were mixed with the PLA-PTES network precursor during acidic hydrolysis step. Upon evaporation, the silanol groups carried by peptides crosslinked with the silyl groups of the extremities of the PLA resulting in a hybrid peptide-PLA network. As proof of concept, we first synthesized a model hybrid peptide (**peptide 1**) that carry two triethoxysilyl groups at the N- and C-terminus and that modeled the identified bioactive **peptide 2**. The C-terminus was coupled to a diamino spacer to generate an additional amino group and allow its functionalization (**Scheme 1**). It should be noted that **peptide 1** was fluorescent to facilitate its detection within the polymer network. **Peptide 1** was added (0.1 % molar) to PLA-12k-PTES, selected for its low Young's modulus, resulting in a homogeneous hybrid peptide PLA film (PLA-12k-PTES **3c**-0.1% **peptide 1**). To prove the covalent incorporation of the peptide, PLA-12k-PTES **3c**-10% **peptide 1** films were immersed into dichloromethane for 3 hours. As expected, fluorescence was maintained in the insoluble fraction, witnessing that the peptide entered covalently in the composition of the network (**Supporting Information, Figure S8**).

We questioned what would be the impact of introducing a peptide on the mechanical properties of the hybrid peptide-PLA film. The peptide PLA film proved to be more rigid and more resistant at failure compared to the crosslinked films without peptide. Correspondingly, as shown in **Table 2**, the introduction of **Peptide 1** at a ratio of 0.1% resulted in a 4-fold increase of E (from 1.0 ± 0.5 MPa to 3.8 ± 0.7 MPa) and a 36-fold increase of the stress at failure (from 5 ± 1 kPa to 178 ± 25 MPa), whereas the strain at failure were 3-fold decreased (from 28.7 % to 9.9 %) compared to the films obtained only with PLA-12k-PTES **3c**. This is explained by the formation of new Si-O-Si bonds between the peptide and the functionalized polymers and is illustrated by the increase in the percentage of gel fraction from 30% to 82% after the introduction of 0.1% molar of **peptide 1** for the same amount of PLA-12k PTES **3c** (**Table 2**).

Then, we studied the impact of the molecular weight of the star-PLA-PTES and the introduction of the peptide **1** on the degradation of the network. Due to the insolubility of films, it was not possible to evaluate the network degradation by monitoring the evolution of M_n with SEC. Thus, the degradability of the different samples was studied by evaluation of the gel fraction and the mass loss percentage measurement after different immersion times in phosphate buffer solution (PBS) simulating physiological medium at 37°C. (**Figure 5A** and **Figure 5B**). Polymers networks were quite stable after 8 weeks. Indeed, the gel fractions slowly varied from 98 % to 88 % (for networks obtained with from Star-PLA-2k-PTES **3a**) and from 30 % to 14 % (for networks obtained from Star-PLA-12k-PTES **3c**). In spite of this decrease in gel fraction which implies chain hydrolysis of PLA or siloxanes, we noted that the mass loss was slight suggesting that materials were still in an early degradation stage (**Figure 5B**). However, the introduction of **Peptide-1** led to a significant decrease of the gel fraction (54% initially to 15% after 8 weeks) compared to the functionalized PLA **3c** without peptide (30% initially to 12% after 8 weeks)

(**Figure 5C**). It has been shown that silanes could hydrolyze rapidly in water at pH 7.^{35,36} Since the presence of the peptide increases the number of Si-O-Si bonds in the PLA-peptide network, it can then be expected that this network degrades faster than the PLA network without peptide. Despite the decrease of the crosslinking rate brought by the peptide, the limited samples weight loss (4 % after 1 week and 7 % after 8 weeks) showed that samples were still at the early stage of their degradation (**Figure 5D**).

We also evaluated the impact of **Peptide-1** on the evolution of mechanical properties under simulated biological conditions at 37°C over 8 weeks (**Figure 5E**). While the gel fraction drastically dropped during the degradation time, we observed that the Young's modulus and the stress required to break the star-shaped PLA-**Peptide-1** hybrid networks slowly decreased over 8 weeks. Indeed, the Young's modulus decreased from 6.01 ± 0.02 MPa to 1.73 ± 0.02 MPa after 8 weeks of degradation and the stress at failure ranged from 0.17 ± 0.07 MPa to 0.10 ± 0.01 MPa (**Figure 5F**).

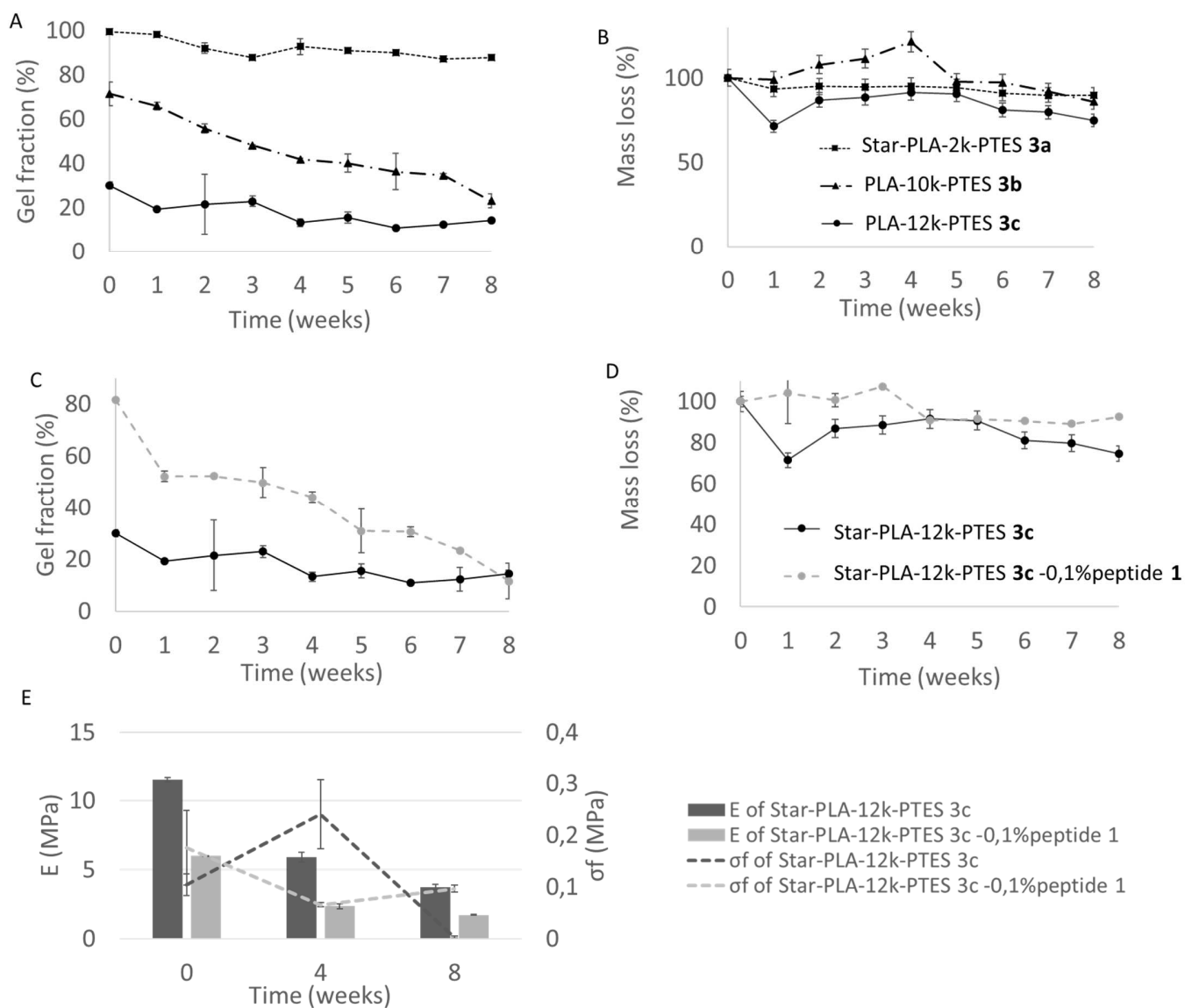


Figure 5. Degradation studies of PLA and PLA-peptide hybrid networks: (A,B) Influence of Star-PLA molecular weight on network gel fraction and mass loss evolution by comparing films obtained from Star-PLA **3a**, **3b** and **3c**. (C,D,E) Peptide introduction impact on networks: gel fraction, mass loss and evolution of mechanical properties. Comparison of materials obtained from star PLA-PTES **3c** and **3c** + 1% molar of Peptide **1**. (no color needed)

Having demonstrated the easiness of functionalization and the relative stability of resulting PLA peptide materials obtained by sol-gel, we evaluated the biological properties of a novel star PLA-PTES based material incorporating a laminin sequence IKVAV whose effect on fibroblast adhesion is documented in the literature.^{37,38,39} Consequently, we synthesized silylated **peptide 2** which included the IKVAV sequence, functionalized in the same way than **peptide 1**, at both extremities by IPTES. Star-PLA-PTES **3c**-Peptide **2** films have been prepared in the same way as described above with **peptide 1**. We first checked the cytotoxicity of the resulting hybrid PLA-peptide film according to ISO 10993-12 standard. Briefly Star-PLA-PTES **3c** and Peptide **2** were put in contact with L929 cells layer. After 24 hours, cell viability was evaluated by measuring mitochondrial activity in the cells (**Figure 6A**). The percentage of cell viability was higher than 70 % of the viability obtained on high density polyethylene film (positive control), indicating that both Star-PLA-12k-PTES **3c** and Peptide **2** present a very low cytotoxicity.

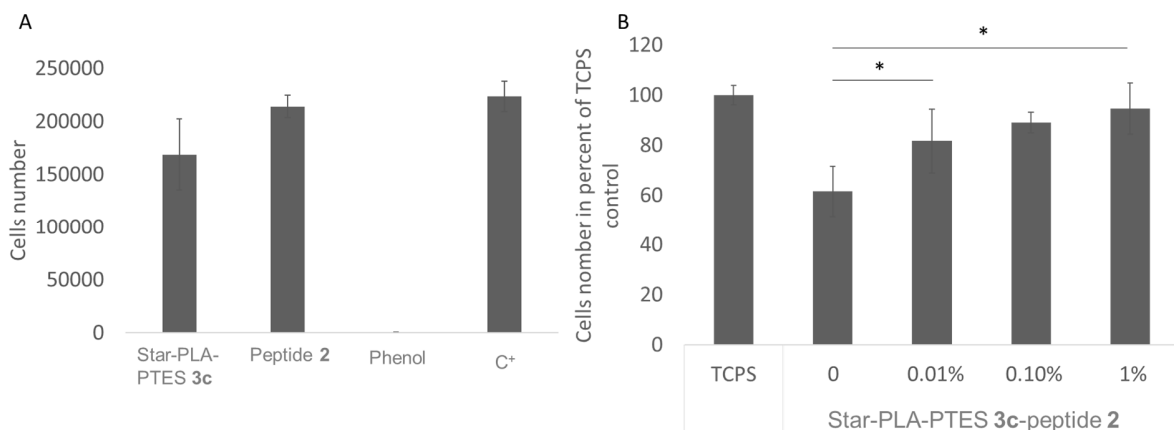


Figure 6. Biological activity of materials Star-PLA-PTES **3c** and Peptide **2**. (A) Viability of L929 cells, phenol as negative control and high-density polyethylene film as positive control. (B) Adhesion of L929 cells after 4h on Star-PLA-PTES **3c**-peptide **2** that contained 0, 0.01 %, 0.1 % and 1% of peptide **2** and on treated for cells polystyrene surface (TCPS) as positive control.

Results are presented as a mean of 3 experiments and error bars represent SD, *p <0.05 (Non-parametric Mann-Whitney test). (no color needed)

Cell adhesion was evaluated by counting the number of cells that adhered to Star-PLA-PTES **3c**-peptide **2** films that contained 0, 0.01 %, 0.1 % and 1% of peptide **2**. As expected, increased amounts of peptide **2** in PLA-12k-PTES-peptide **2** network films improved significantly the cellular adhesion. Indeed, the variation of peptide quantity from 0.01 % to 1 % led to adhesion between 80 % and 95 % compared to cell-treated polystyrene surfaces (**Figure 6B**). The introduction of a very small quantity of peptide (between 0.3 and 3 mg, i.e. between 0.16 and 1.58 mg of peptide / cm² of biomaterials surface area) thus lead to an increase of 20.2% to 33.1% of the cell adhesion. It has been shown that a coating of 0.31 mg IKVAV per cm² surface area of a glass plate improves NHDF proliferation by 10%.³⁹ The same percentage increase in adhesion of PC-12 cells was observed in a three-dimensional environment, i.e. on PLA nanofibers grafted by the IKVAV sequence.⁴⁰ This show that the sequence covalently incorporated into a three-dimensional polymer network have an efficiency on cell adhesion similar or even superior to what is described in the literature.

4 Conclusions

For the first time, we demonstrated that poly(lactide), a polymer widely used for biomedical application could be crosslinked using sol-gel siloxane chemistry, yielding networks with tunable properties. By modulating the molecular weight of the star-PLA, loose or tight networks could be obtained with controllable mechanical properties. Besides this new type of inorganic-polymeric chemical network, we took profit of the modularity of the sol-gel process to introduce, in a single

step, silylated peptides. Thanks to triethoxysilyl moieties, these hybrid molecules took part covalently in the 3D network. Such hybrid networks kept stable mechanical properties over 8 weeks in an aqueous environment. We also showed that when bioactive sequences are used, the resulting hybrid network displayed interesting biological properties. As a first example, laminin-derived IKVAV sequence increased the adhesion properties of the cells. It is worth highlighting that besides cell-adhesive sequences, any other types of bioactive peptides or even drugs or other biopolymers ^{30,31,33} could be also added to give targeted properties to the PLA based materials, as far as they bear one or several triethoxysilyl groups. An interesting perspective would be to consider the complexity of tissues in the shaping of this material. Indeed, this work paves the way to the tailorable design of a wide range of materials which could be shaped as nanofibres, microparticles or used as bioinks for 3D printing. ^{29,33}

TABLE OF CONTENTS

Figure 1. Silylated star-PLA and hybrid silylated star-PLA-peptide networks formation by sol-gel process.

Figure 2. Peptide 1

Figure 3. Peptide 2

Figure 4. General synthesis of tetra(triethoxysilyl) star-PLA

Table 1. ¹H-NMR and SEC characterizations of star-PLA and tetrafunctionalized star-PLA

Table 2 Mechanical properties at 37°C of PLA-PTES films and PLA-PTES-peptide hybrid films: the mean value of Young's Modulus (E, MPa), stress at failure (σ_f , kPa) and strain at failure (ϵ_f , %)

Figure 5. Degradation studies of PLA and PLA-peptide hybrid networks: (A,B) Influence of Star-PLA molecular weight on network gel fraction and mass loss evolution by comparing films obtained from Star-PLA **3a**, **3b** and **3c**. (C,D,E) Peptide introduction impact on networks: gel fraction, mass loss and evolution of mechanical properties. Comparison of materials obtained from star PLA-PTES **3c** and **3c** + 1% molar of Peptide **1**

Figure 6. Biological activity of materials Star-PLA-PTES **3c** and Peptide **2**. (A) Viability of L929 cells, phenol as negative control and high-density polyethylene film as positive control. (B) Adhesion of L929 cells after 4h on Star-PLA-PTES **3c**-peptide **2** that contained 0, 0.01 %, 0.1 % and 1% of peptide **2** and on treated cells polystyrene surface (TCPS) as positive control. Results are presented as a mean of 3 experiments and error bars represent SD, *p <0.05 (Non-parametric Mann-Whitney test).

AUTHOR INFORMATION

Corresponding Author

* E-mail: coline.pinese@umontpellier.fr

* Faculty of pharmacy, 15 avenue Charles Flahault, 34090 Montpellier

ACKNOWLEDGMENT

Peptide syntheses and polymers characterization were performed using the facilities of SynBio3 IBISA platform supported by ITMO cancer.

DATA AVAILABILITY

The raw/processed data required to reproduce these findings cannot be shared at this time due to technical or time limitations

REFERENCES

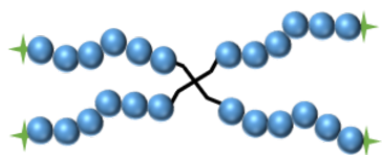
- (1) Boccaccini, A. R.; Blaker, J. J. Bioactive Composite Materials for Tissue Engineering Scaffolds. *Expert Rev. Med. Devices* **2005**, *2* (3), 303–317. <https://doi.org/10.1586/17434440.2.3.303>.
- (2) Guo, B.; Lei, B.; Li, P.; Ma, P. X. Functionalized Scaffolds to Enhance Tissue Regeneration. *Regen. Biomater.* **2015**, *2* (1), 47–57. <https://doi.org/10.1093/rb/rbu016>.
- (3) Bramhill, J.; Ross, S.; Ross, G. Bioactive Nanocomposites for Tissue Repair and Regeneration: A Review. *Int. J. Environ. Res. Public Health* **2017**, *14* (1), 66. <https://doi.org/10.3390/ijerph14010066>.
- (4) “Click” Chemistry in Polymeric Scaffolds: Bioactive Materials for Tissue Engineering. *J. Controlled Release* **2018**, *273*, 160–179. <https://doi.org/10.1016/j.jconrel.2018.01.023>.
- (5) Webb, A. R.; Yang, J.; Ameer, G. A. Biodegradable Polyester Elastomers in Tissue Engineering. *Expert Opin. Biol. Ther.* **2004**, *4* (6), 801–812. <https://doi.org/10.1517/14712598.4.6.801>.
- (6) Pinese, C.; Leroy, A.; Nottelet, B.; Gagnieu, C.; Coudane, J.; Garric, X. Rolled Knitted Scaffolds Based on PLA-Pluronic Copolymers for Anterior Cruciate Ligament Reinforcement: A Step by Step Conception. *J. Biomed. Mater. Res. B Appl. Biomater.* **2017**, *105* (4), 735–743. <https://doi.org/10.1002/jbm.b.33604>.
- (7) Singhvi, M. S.; Zinjarde, S. S.; Gokhale, D. V. Polylactic Acid: Synthesis and Biomedical Applications. *J. Appl. Microbiol.* **2019**, *127* (6), 1612–1626. <https://doi.org/10.1111/jam.14290>.
- (8) Saini, P.; Arora, M.; Kumar, M. N. V. R. Poly(Lactic Acid) Blends in Biomedical Applications. *Adv. Drug Deliv. Rev.* **2016**, *107*, 47–59. <https://doi.org/10.1016/j.addr.2016.06.014>.
- (9) Harrane, A.; Leroy, A.; Nouailhas, H.; Garric, X.; Coudane, J.; Nottelet, B. PLA-Based Biodegradable and Tunable Soft Elastomers for Biomedical Applications. *Biomed. Mater.* **2011**, *6* (6), 065006. <https://doi.org/10.1088/1748-6041/6/6/065006>.
- (10) Rasal, R. M.; Janorkar, A. V.; Hirt, D. E. Poly(Lactic Acid) Modifications. *Progress in Polymer Science (Oxford)*. March 2010, pp 338–356. <https://doi.org/10.1016/j.progpolymsci.2009.12.003>.
- (11) Pinese, C.; Lin, J.; Milbreta, U.; Li, M.; Wang, Y.; Leong, K. W.; Chew, S. Y. Sustained Delivery of siRNA/Mesoporous Silica Nanoparticle Complexes from Nanofiber Scaffolds for Long-Term Gene Silencing. *Acta Biomater.* **2018**, *76*, 164–177. <https://doi.org/10.1016/j.actbio.2018.05.054>.
- (12) Zhang, N.; Milbreta, U.; Chin, J. S.; Pinese, C.; Lin, J.; Shirahama, H.; Jiang, W.; Liu, H.; Mi, R.; Hoke, A.; Wu, W.; Chew, S. Y. Biomimicking Fiber Scaffold as an Effective In Vitro and In Vivo MicroRNA Screening Platform for Directing Tissue Regeneration. *Adv. Sci.* *0* (0), 1800808. <https://doi.org/10.1002/advs.201800808>.
- (13) Canalle, L. A.; Löwik, D. W. P. M.; Hest, J. C. M. van. Polypeptide–Polymer Bioconjugates. *Chem. Soc. Rev.* **2009**, *39* (1), 329–353. <https://doi.org/10.1039/B807871H>.

- (14) Shu, J. Y.; Panganiban, B.; Xu, T. Peptide-Polymer Conjugates: From Fundamental Science to Application. *Annu. Rev. Phys. Chem.* **2013**, *64*, 631–657. <https://doi.org/10.1146/annurev-physchem-040412-110108>.
- (15) Callahan, L. A. S.; Xie, S.; Barker, I. A.; Zheng, J.; Reneker, D. H.; Dove, A. P.; Becker, M. L. Directed Differentiation and Neurite Extension of Mouse Embryonic Stem Cell on Aligned Poly(Lactide) Nanofibers Functionalized with YIGSR Peptide. *Biomaterials* **2013**, *34* (36), 9089–9095. <https://doi.org/10.1016/j.biomaterials.2013.08.028>.
- (16) DeForest, C. A.; Polizzotti, B. D.; Anseth, K. S. Sequential Click Reactions for Synthesizing and Patterning Three-Dimensional Cell Microenvironments. *Nat. Mater.* **2009**, *8* (8), 659–664. <https://doi.org/10.1038/nmat2473>.
- (17) Samad, A. A.; Bethry, A.; Janouskova, O.; Ciccione, J.; Wenk, C.; Coll, J.-L.; Subra, G.; Etrych, T.; Omar, F. E.; Bakkour, Y.; Coudane, J.; Nottelet, B. Iterative Photoinduced Chain Functionalization as a Generic Platform for Advanced Polymeric Drug Delivery Systems. *Macromol. Rapid Commun.* **2018**, *39* (3), 1700502. <https://doi.org/10.1002/marc.201700502>.
- (18) Pauly, A. C.; di Lena, F. Incorporating Amino Acid Sequences into the Backbone Chain of Polymers through Thiol-Ene Chemistry. *Polymer* **2015**, *72*, 378–381. <https://doi.org/10.1016/j.polymer.2015.02.022>.
- (19) Anderson, S. B.; Lin, C.-C.; Kuntzler, D. V.; Anseth, K. S. The Performance of Human Mesenchymal Stem Cells Encapsulated in Cell-Degradable Polymer-Peptide Hydrogels. *Biomaterials* **2011**, *32* (14), 3564–3574. <https://doi.org/10.1016/j.biomaterials.2011.01.064>.
- (20) Phelps, E. A.; Enemchukwu, N. O.; Fiore, V. F.; Sy, J. C.; Murthy, N.; Sulchek, T. A.; Barker, T. H.; García, A. J. Maleimide Cross-Linked Bioactive PEG Hydrogel Exhibits Improved Reaction Kinetics and Cross-Linking for Cell Encapsulation and in Situ Delivery. *Adv. Mater. Deerfield Beach Fla* **2012**, *24* (1), 64–70, 2. <https://doi.org/10.1002/adma.201103574>.
- (21) Phelps, E. A.; Templeman, K. L.; Thulé, P. M.; García, A. J. Engineered VEGF-Releasing PEG-MAL Hydrogel for Pancreatic Islet Vascularization. *Drug Deliv. Transl. Res.* **2015**, *5* (2), 125–136. <https://doi.org/10.1007/s13346-013-0142-2>.
- (22) Lutolf, M. P.; Lauer-Fields, J. L.; Schmoekel, H. G.; Metters, A. T.; Weber, F. E.; Fields, G. B.; Hubbell, J. A. Synthetic Matrix Metalloproteinase-Sensitive Hydrogels for the Conduction of Tissue Regeneration: Engineering Cell-Invasion Characteristics. *Proc. Natl. Acad. Sci. U. S. A.* **2003**, *100* (9), 5413–5418. <https://doi.org/10.1073/pnas.0737381100>.
- (23) Park, Y.; Lutolf, M. P.; Hubbell, J. A.; Hunziker, E. B.; Wong, M. Bovine Primary Chondrocyte Culture in Synthetic Matrix Metalloproteinase-Sensitive Poly(Ethylene Glycol)-Based Hydrogels as a Scaffold for Cartilage Repair. *Tissue Eng.* **2004**, *10* (3–4), 515–522. <https://doi.org/10.1089/107632704323061870>.
- (24) Cellesi, F.; Tirelli, N.; Hubbell, J. A. Towards a Fully-Synthetic Substitute of Alginate: Development of a New Process Using Thermal Gelation and Chemical Cross-Linking. *Biomaterials* **2004**, *25* (21), 5115–5124. <https://doi.org/10.1016/j.biomaterials.2003.12.015>.
- (25) Echalié, C.; Pinese, C.; Garric, X.; Van Den Berghe, H.; Jumas Bilak, E.; Martínez, J.; Mehdi, A.; Subra, G. Easy Synthesis of Tunable Hybrid Bioactive Hydrogels. *Chem. Mater.* **2016**, *28* (5), 1261–1265. <https://doi.org/10.1021/acs.chemmater.5b04881>.

- (26) Echali er, C.; Levato, R.; Mateos-Timoneda, M. A.; Casta no, O.; D ejean, S.; Garric, X.; Pinese, C.; No el, D.; Engel, E.; Martinez, J.; Mehdi, A.; Subra, G. Modular Bioink for 3D Printing of Biocompatible Hydrogels: Sol–Gel Polymerization of Hybrid Peptides and Polymers. *RSC Adv.* **2017**, *7* (20), 12231–12235. <https://doi.org/10.1039/C6RA28540F>.
- (27) Guillaume, S. M. Advances in the Synthesis of Silyl-Modified Polymers (SMPs). *Polymer Chemistry*. Royal Society of Chemistry April 21, 2018, pp 1911–1926. <https://doi.org/10.1039/c8py00265g>.
- (28) Jebors, S.; Enjalbal, C.; Amblard, M.; Mehdi, A.; Subra, G.; Martinez, J. Bioorganic Hybrid OMS by Straightforward Grafting of Trialkoxysilyl Peptides. *J. Mater. Chem. B* **2013**, *1* (23), 2921–2925. <https://doi.org/10.1039/C3TB20122H>.
- (29) Ciccione, J.; Jia, T.; Coll, J.-L.; Parra, K.; Amblard, M.; Jebors, S.; Martinez, J.; Mehdi, A.; Subra, G. Unambiguous and Controlled One-Pot Synthesis of Multifunctional Silica Nanoparticles. *Chem. Mater.* **2016**, *28* (3), 885–889. <https://doi.org/10.1021/acs.chemmater.5b04398>.
- (30) Pinese, C.; Jebors, S.; Echali er, C.; Licznar-Fajardo, P.; Garric, X.; Humblot, V.; Calers, C.; Martinez, J.; Mehdi, A.; Subra, G. Simple and Specific Grafting of Antibacterial Peptides on Silicone Catheters. *Adv. Healthc. Mater.* **2016**, *5* (23), 3067–3073. <https://doi.org/10.1002/adhm.201600757>.
- (31) Pinese, C.; Jebors, S.; Stoebner, P. E.; Humblot, V.; Verdi e, P.; Causse, L.; Garric, X.; Taillades, H.; Martinez, J.; Mehdi, A.; Subra, G. Bioactive Peptides Grafted Silicone Dressings: A Simple and Specific Method. *Mater. Today Chem.* **2017**, *4*, 73–83. <https://doi.org/10.1016/j.mtchem.2017.02.007>.
- (32) Jebors, S.; Ciccione, J.; Al-Halifa, S.; Nottelet, B.; Enjalbal, C.; M’Kadmi, C.; Amblard, M.; Mehdi, A.; Martinez, J.; Subra, G. A New Way to Silicone-Based Peptide Polymers. *Angew. Chem. Int. Ed.* **2015**, *54* (12), 3778–3782. <https://doi.org/10.1002/anie.201411065>.
- (33) Echali er, C.; Jebors, S.; Laconde, G.; Brunel, L.; Verdi e, P.; Causse, L.; Bethry, A.; Legrand, B.; Van Den Berghe, H.; Garric, X.; No el, D.; Martinez, J.; Mehdi, A.; Subra, G. Sol–Gel Synthesis of Collagen-Inspired Peptide Hydrogel. *Mater. Today* **2017**, *20* (2), 59–66. <https://doi.org/10.1016/j.mattod.2017.02.001>.
- (34) Wojtczak, E.; Kubisa, P.; Bednarek, M. Thermal Stability of Polylactide with Different End-Groups Depending on the Catalyst Used for the Polymerization. *Polym. Degrad. Stab.* **2018**, *151*, 100–104. <https://doi.org/10.1016/j.polymdegradstab.2018.03.003>.
- (35) Xiao, S.-J.; Textor, M.; Spencer, N. D.; Sigrist, H. Covalent Attachment of Cell-Adhesive, (Arg-Gly-Asp)-Containing Peptides to Titanium Surfaces. *Langmuir* **1998**, *14* (19), 5507–5516. <https://doi.org/10.1021/la980257z>.
- (36) Iorio, M.; Olmos, D.; Santarelli, M. L.; Gonz alez-Benito, J. Fluorescence Study of the Hydrolytic Degradation Process of the Polysiloxane Coatings of Basalt Fibers. *Appl. Surf. Sci.* **2019**, *475*, 754–761. <https://doi.org/10.1016/j.apsusc.2018.12.223>.
- (37) Hassanisaber, H.; Jafari, L.; Campeau, M. A.; Drevelle, O.; Lauzon, M. A.; Langelier, E.; Fauchoux, N.; Rouleau, L. The Effect of Substrate Bulk Stiffness on Focal and Fibrillar Adhesion Formation in Human Abdominal Aortic Endothelial Cells. *Mater. Sci. Eng. C* **2019**, *98*, 572–583. <https://doi.org/10.1016/j.msec.2018.12.130>.
- (38) Yergoz, F.; Hastar, N.; Cimenci, C. E.; Ozkan, A. D.; Tekinay, T.; Guler, M. O.; Tekinay, A. B. Heparin Mimetic Peptide Nanofiber Gel Promotes Regeneration of Full Thickness Burn Injury. *Biomaterials* **2017**, *134*, 117–127. <https://doi.org/10.1016/j.biomaterials.2017.04.040>.

- (39) Hashimoto, T.; Suzuki, Y.; Tanihara, M.; Kakimaru, Y.; Suzuki, K. Development of Alginate Wound Dressings Linked with Hybrid Peptides Derived from Laminin and Elastin. *Biomaterials* **2004**, *25* (7–8), 1407–1414. <https://doi.org/10.1016/j.biomaterials.2003.07.004>.
- (40) Hsu, Y.-I.; Yamaoka, T. Improved Exposure of Bioactive Peptides to the Outermost Surface of the Polylactic Acid Nanofiber Scaffold. *J. Biomed. Mater. Res. B Appl. Biomater.* **2020**, *108* (4), 1274–1280. <https://doi.org/10.1002/jbm.b.34475>.

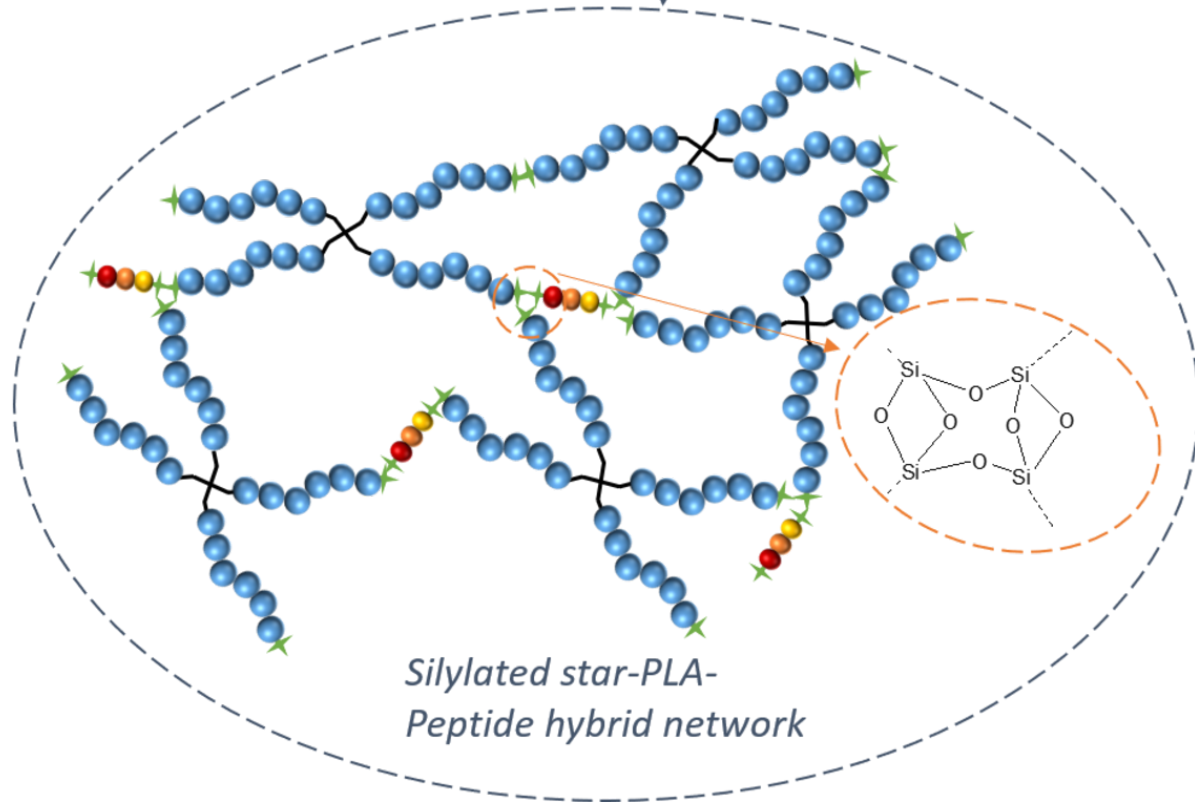
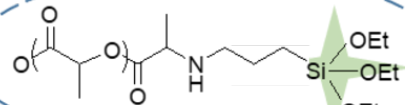
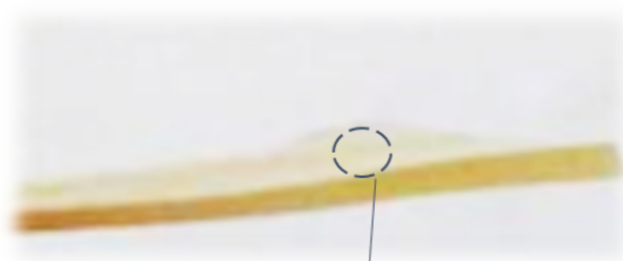
Tetrafunctional Star-PLA



Bifunctional bioactive peptide



Bioactive hybrid networks for soft tissue reconstruction



*Silylated star-PLA-
Peptide hybrid network*